

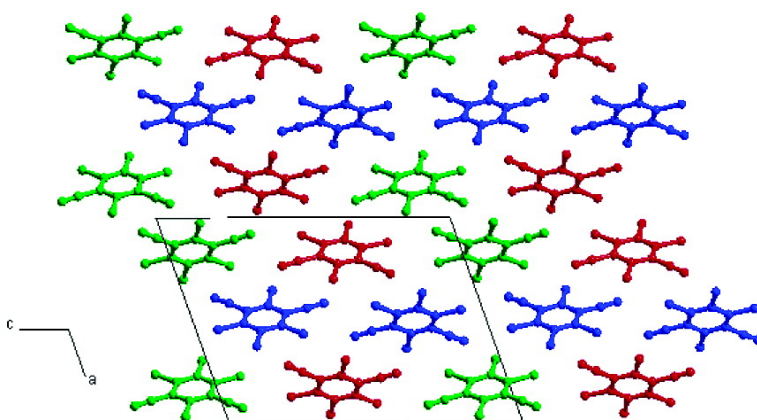
Article

Characterization of Complicated New Polymorphs of Chlorothalonil by X-ray Diffraction and Computer Crystal Structure Prediction

Maryjane Tremayne, Leanne Grice, James C. Pyatt, Colin C. Seaton, Benson M. Kariuki, Helen H. Y. Tsui, Sarah L. Price, and Julian C. Cherryman

J. Am. Chem. Soc., **2004**, 126 (22), 7071-7081 • DOI: 10.1021/ja0498235 • Publication Date (Web): 12 May 2004

Downloaded from <http://pubs.acs.org> on March 31, 2009



More About This Article

Additional resources and features associated with this article are available within the HTML version:

- Supporting Information
- Links to the 2 articles that cite this article, as of the time of this article download
- Access to high resolution figures
- Links to articles and content related to this article
- Copyright permission to reproduce figures and/or text from this article

[View the Full Text HTML](#)



Characterization of Complicated New Polymorphs of Chlorothalonil by X-ray Diffraction and Computer Crystal Structure Prediction

Maryjane Tremayne,^{*,†} Leanne Grice,[†] James C. Pyatt,[†] Colin C. Seaton,[†] Benson M. Kariuki,[†] Helen H. Y. Tsui,[‡] Sarah L. Price,[‡] and Julian C. Cherryman[§]

Contribution from the School of Chemistry, University of Birmingham, Edgbaston, Birmingham, B15 2TT, U.K., Centre for Theoretical and Computational Chemistry, Department of Chemistry, University College London, 20 Gordon Street, London, WC1H 0AJ, U.K., and Avecia Limited, P.O. Box 24, Hexagon House, Blackley, Manchester, M9 8ZS, U.K.

Received January 11, 2004; E-mail: m.tremayne@bham.ac.uk

Abstract: A simultaneous experimental and computational search for polymorphs of chlorothalonil (2,4,5,6-tetrachloro-1,3-benzenedicarbonitrile) has been conducted, leading to the first characterization of forms 2 and 3. The crystal structure prediction study, using a specifically developed anisotropic atom–atom potential for chlorothalonil, gave as the global minimum in the lattice energy a structure that was readily refined against powder diffraction data to the known form 1 ($P2_1/a$). The structure of form 2 was solved and refined from powder diffraction data, giving a disordered structure in the $R\bar{3}m$ (166) space group ($Z = 3$). It could also be refined against a $P\bar{1}$ ordered model, starting from a low-energy hypothetical sheet structure found in the computational search. This shows that the disorder could be associated with the stacking of ordered sheets. The disordered structure for form 2 was later confirmed by single-crystal X-ray diffraction. The structure of form 3, determined from single-crystal diffraction, contains three independent molecules in the asymmetric unit in $P2_1$ (4) ($Z = 6$). Powder diffraction showed that this single-herringbone structure was similar to two low-energy structures found in the search. Further analysis confirmed that form 3 has a similar lattice energy and contains elements from both these predicted structures, which can be considered as good approximations to the form 3 structure.

Introduction

Polymorphism, the ability to adopt more than one crystal structure,¹ is of major concern to both pharmaceutical and agrochemical development because of the need to control the polymorphic form produced. The considerable variation in properties between different polymorphs makes the characterization of all polymorphic forms essential for the full structural understanding of any molecular material.

One such system is chlorothalonil (2,4,5,6-tetrachloro-1,3-benzenedicarbonitrile), a general-use pesticide commonly known under the trade names Bravo or Daconil 2787 that is used as a broad-spectrum fungicide on both horticultural crops² and in home gardens and as a biocide in paints and wood preservatives. The commercially available form (form 1) remains stable over time and has been fully structurally characterized.³ However, the patent⁴ for chlorothalonil indicates the possibility of another polymorphic form that shows a reduced biological activity and

undergoes irreversible hardening in production, although there is no reliable crystallographic information regarding this second form.

Hence, a simultaneous theoretical prediction and experimental search for new polymorphs of chlorothalonil was carried out. Initially this was done independently, so that it would be a test of crystal structure prediction methods if all the polymorphs could be characterized independently from single crystal or powder X-ray diffraction data. If the new polymorphs could not be characterized in this way, it was hoped that we would be able to select possible polymorphs from the predicted structures and use these as a starting point for Rietveld refinement.

Computational crystal structure prediction aims to propose the crystal structures of organic molecules from their chemical structure. There have been many successes,⁵ including in blind tests,⁶ based on searching for the global minimum in the lattice energy. However, such searches usually find many more energetically feasible crystal structures than known (or likely) polymorphs. The great challenge to crystal structure prediction is to determine which of these low-energy structures are likely to be observed polymorphs. Initial attempts to improve the

[†] University of Birmingham.

[‡] University College London.

[§] Avecia Limited.

(1) Bernstein, J. *Polymorphism in Molecular Crystals*; IUCr Monographs on Crystallography 14; Oxford University Press: New York, 2002.

(2) *Farm Chemicals Handbook 2002: Global Guide to Crop Protection*; Meister Publishing: Willoughby, OH, 2002.

(3) Britton, D. *Cryst. Struct. Commun.* **1981**, *10*, 1501.

(4) Querzola, G.; Epis, G. Production Process of Chlorothalonil. Patent WO 86/06066, 1986.

(5) Beyer, T.; Lewis, T.; Price, S. L. *CrystEngComm* **2001**, *44*, 178. <http://www.rsc.org/CrystEngComm>.

thermodynamic model by considering the effects of lattice vibrations⁷ or eliminating structures whose crystallites are estimated to be too mechanically weak or slow-growing with extreme plate or needlelike morphologies⁸ have somewhat reduced the number of feasible polymorphs in preliminary applications. Thus chlorothalonil, which is known to be polymorphic, provides a test of whether the computational approach can generate the observed structures as the most probable polymorphs. Even if this ambitious aim is not achieved, the set of energetically feasible hypothetical structures should include any ordered experimental structures within the range of space groups and Z' values covered by the search. The corresponding hypothetical structures should be recognizable from the experimental powder diffraction patterns and be sufficiently accurate so as to be adequate starting points for Rietveld refinement of the crystal structures from the powder diffraction data.

The chlorothalonil molecule provides a novel challenge to crystal structure prediction, because the dominant Cl...N interactions are directional,⁹ with significant anisotropy in the shape of the repulsive wall, mainly due to the nonspherical charge distribution around the chlorine nucleus. Thus, a specific anisotropic atom-atom repulsion potential was developed for chlorothalonil, by using a novel nonempirical method that has been applied to cyanuric chloride¹⁰ and chlorobenzenes.¹¹ This anisotropic repulsion potential, in conjunction with a distributed multipole electrostatic and nonempirical dispersion model potential, was used to refine the low-energy crystal structures generated by using an empirical repulsion-dispersion model potential. This alternative specific model potential, which reflects the anisotropic shape of the atoms, required a considerable effort to develop but has the advantage that the use of two different model potentials, based on different assumptions, provides considerable confidence in the relative lattice energies of the known and hypothetical structures.

A potential use of the crystal structures generated in a prediction is to help characterize new polymorphs by matching experimental powder diffraction data to that calculated from these calculated structures. However, this is often done visually or purely on a fingerprinting basis, and there are only a few molecular cases in which the predicted structures have been used as a starting point for Rietveld refinement¹² both in terms of lattice parameters and crystal structure. Although the development of direct-space methods of structure solution has led to considerable advances in the use of X-ray powder diffraction data for ab initio structure determination of organic molecular solids,¹³ these methods still require prior knowledge

of lattice parameters (usually obtained via indexing procedures) before structure solution can be attempted. The use of structure prediction to supply both lattice and structural information can enable successful structural characterization when the powder data itself is not ideal and the indexing procedures fail. However, in this situation Rietveld refinement becomes more complicated and can easily converge to an incorrect local minimum despite the results from the structure prediction being within a few percent of the final refined lattice parameters.^{12a}

In this article, we report the first successful prediction (and subsequent Rietveld refinement) of three polymorphs of a substance (within constraints of prediction techniques), with two new polymorphs uncharacterized before prediction. In the event, the powder pattern of form 2 made it obvious that the structure was so highly symmetrical that it must be disordered, and is therefore of a type that could not be predicted by current theoretical methods. The determination of this disordered crystal structure from powder data also turned out to be more problematical than expected because of detrimental sample effects and clearly illustrates that the solution of seemingly trivial structures in terms of global optimization direct-space techniques is not always straightforward. Refinements based on the hypothetical structures predicted in the search facilitated an interpretation of this disorder. The presence of multiple molecules in the asymmetric unit of form 3 presents another structure that could not be predicted by current theoretical methods. However, the search did locate two hypothetical structures that clearly show significant similarities to the form 3 structure. Rietveld refinement of these predicted structures, which are clearly only approximations to the true structure, warns against over-interpretation of the powder data in the case of a structure that at first glance is not overly complex.

Thus, the structural characterization and rationalization of these new polymorphs of chlorothalonil has required multidisciplinary innovation between theoretical prediction and experimental methods, with both approaches generating structural information that could not have been obtained without the complementary use of these techniques.

Experimental Section

Sample Preparation. Chlorothalonil form 1 was used directly as received (Aldrich). Forms 2 and 3 were prepared from commercial chlorothalonil (Aldrich) recrystallized by slow cooling from butanol and ethyl acetate, respectively. In both cases, small white crystallites of chlorothalonil were obtained (elemental analysis showed form 2: C, 36.2; N, 10.1; H, 0.0% and form 3: C, 37.3; N, 10.8; H, 0.0%; calcd for C₈Cl₄N₂: C, 36.1; N, 10.5; H, 0.0%). X-ray powder diffraction was used to confirm that new polymorphs had been prepared, although it was clear that the sample of form 3 also contained a small amount of form 1.

X-ray Powder Diffraction Measurements. X-ray powder diffraction data were collected on a high-resolution Bruker AXS D5000 diffractometer using Ge-monochromated Cu K α_1 radiation ($\lambda = 1.54056$ Å) and a position-sensitive detector covering 8° in 2θ . Data were recorded in transmission mode using a flat disc, with the sample placed between two pieces of tape, over the range $10^\circ \leq 2\theta \leq 55^\circ$ for 1 h (forms 1 and 2) in 0.01925° steps and over the range $12^\circ \leq 2\theta \leq 85^\circ$

- (6) (a) Lommerse, J. P. M.; Motherwell, W. D. S.; Ammon, H. L.; Dunitz, J. D.; Gavezzotti, A.; Hofmann, D. W. M.; Leusen, F. J. J.; Mooij, W. T. M.; Price, S. L.; Schweizer, B.; Schmidt, M. U.; van Eijck, B. P.; Verwer, P.; Williams, D. E. *Acta Crystallogr., Sect. B* **2000**, *56*, 697. (b) Motherwell, W. D. S.; Ammon, H. L.; Dunitz, J. D.; Dzyabchenko, A.; Erk, P.; Gavezzotti, A.; Hofmann, D. W. M.; Leusen, F. J. J.; Lommerse, J. P. M.; Mooij, W. T. M.; Price, S. L.; Scheraga, H.; Schweizer, B.; Schmidt, M. U.; van Eijck, B. P.; Verwer, P.; Williams, D. E. *Acta Crystallogr., Sect. B* **2002**, *58*, 348.
- (7) van Eijck, B. P. *J. Comput. Chem.* **2001**, *22*, 816.
- (8) Beyer, T.; Day, G. M.; Price, S. L. *J. Am. Chem. Soc.* **2001**, *123*, 5086.
- (9) Lommerse, J. P. M.; Stone, A. J.; Taylor, R.; Allen, F. H. *J. Am. Chem. Soc.* **1996**, *118*, 3108.
- (10) Mitchell, J. B. O.; Price, S. L.; Leslie, M.; Buttar, D.; Roberts, R. J. *J. Phys. Chem. A* **2001**, *105*, 9961.
- (11) Day, G. M.; Price, S. L. *J. Am. Chem. Soc.* **2003**, *125*, 16343.
- (12) (a) Karfunkel, H. R.; Wu, Z. J.; Burkhard, A.; Rihs, G.; Sinnreich, D.; Buerger, H. M.; Stanek, J. *Acta Crystallogr., Sect. B* **1996**, *52*, 555. (b) Payne, R. S.; Roberts, R. J.; Rowe, R. C.; Docherty, R. *J. Comput. Chem.* **1998**, *19*, 1.

- (13) (a) Harris, K. D. M.; Tremayne, M.; Kariuki, B. M. *Angew. Chem., Int. Ed.* **2001**, *40*, 1626. (b) David, W. I. F.; Shankland, K.; McCusker, L. B.; Baerlocher, C. *Structure Determination from Powder Diffraction Data*; IUCr Monographs on Crystallography 13; Oxford University Press: New York, 2002.

Table 1. Final Refined Parameters and Agreement Factors for the R3m Powder and Single-Crystal Structures, P1 Refinement of the Predicted AB3, and Attempted P1 Ordered Structures of Chlorothalonil Form 2

data	single crystal	powder	powder (AB3)	powder (P1)
a/Å	9.278(4)	9.2392(4)	6.3155(5)	6.3082(5)
b/Å	9.278(4)	9.2392(4)	6.3063(6)	6.2995(4)
c/Å	10.093(3)	10.0969(5)	12.6052(1)	6.3137(5)
α /deg	90	90	94.291(5)	94.202(6)
β /deg	90	90	94.192(6)	94.059(4)
γ /deg	120	120	94.054(5)	94.286(5)
vol/Å ³	752.5(5)	746.4(1)	497.83(8)	248.79(6)
space group	R3m(166)	R3m(166)	P1(2)	P1(1)
Z	3	3	2	1
R _{wp}	0.0609 (R)	0.038	0.036	0.033
R _p		0.025	0.026	0.024
R _{F2}	0.1447 (R _w)	0.074	0.137	0.114
χ^2		3.03	2.22	2.19
pref. orient. [direction]		[001]	[111]	[111]
fraction		0.882	0.960	0.944

for 10 h (form 3). For forms 2 and 3, additional data sets were recorded in capillary geometry (using a 0.5 mm glass capillary filled to a depth of 3 cm). In the case of form 2, these data were collected on a Bruker AXS D5005 diffractometer using Ge-monochromated Cu K α_1 radiation ($\lambda = 1.54056$ Å), whereas for form 3 the data were collected using a high-resolution Bruker AXS D5005 diffractometer, with Gobel mirrors using Cu K $\alpha_{1,2}$ radiation ($\lambda = 1.54184$ Å) with a beam size of 0.6 mm \times 1 cm² and a position sensitive detector with radial slits covering 8° in 2θ .

Single-Crystal X-ray Diffraction Measurements. Data were recorded at 296(2)K on a Rigaku R-Axis IIC diffractometer equipped with a rotating anode source ($\lambda = 0.71069$ Å) and image plate detector system. For form 2, a crystal of size 0.10 \times 0.10 \times 0.15 mm³ was used, and 36 images were recorded as the crystal was rotated through 180° at a crystal-detector distance of 80 mm. For form 3, a crystal of size 0.08 \times 0.08 \times 0.50 mm³ was used. Both structures were solved using SHELXS-86¹⁴ and refined using SHELXL-93.¹⁵ Final crystallographic parameters and agreement factors for forms 2 and 3 are given in Tables 1 and 4, respectively.

Structure Determination of Form 2 from Powder X-ray Diffraction Data. The powder diffraction pattern of form 2 was indexed on the basis of the first 21 observable peaks using the CRYSFIRE package.¹⁶ A large number of cells were obtained with high figures of merit ($M_{20} > 250$),¹⁷ although many of these cells did not satisfy suitable density requirements (often with a volume less than that required for a single chlorothalonil molecule). The unit cell chosen was that of highest symmetry; a trigonal unit cell with hexagonal setting $a = b = 9.24$ Å, $c = 10.10$ Å with a volume 747 Å³ ($Z = 3$). Systematic absences suggested R $\bar{3}$ (148) and R3m (166) as probable space groups, although both would require sixfold symmetry in the molecule. This was possible if the molecule was assumed to be disordered with the $-\text{C}\equiv\text{N}$ and $-\text{Cl}$ substituents on the benzene ring being indistinguishable and represented by a C $-(\text{C}\equiv\text{N})/\text{Cl}$ "spur" (Figure 1). Structure solution was initially attempted in the higher symmetry group R3m.

Because of the symmetry constraints imposed on this structure, the solution was carried out using a grid search technique (implemented in POSSUM¹⁸) by rotation of a C $-(\text{C}\equiv\text{N})/\text{Cl}$ spur with relevant disorder occupancies, around the 0,0,z axis in 1° steps and over the range 0 \leq

$z \leq 0.5$ at intervals of 0.1, thus generating a complete disordered molecular model (Figure 1). Initial attempts at structure solution generated a structure that was clearly incorrect and was immediately rejected as implausible in terms of molecular packing. The rotation of a spur around a fixed axis is a relatively straightforward global optimization problem, and hence, the presence of preferred orientation¹⁹ in the data was investigated as a possible reason for unsuccessful structure solution. Comparison of the original disc data with a data set collected using capillary geometry (Figure 2) clearly showed that the degree of preferred orientation present in this case was severe, and unlike other recent studies²⁰ did not allow direct-space solution of this structure from the worst affected data set. Consequently, structure solution and refinement was carried out using the capillary data, although a preferred orientation correction was still required in refinement.

The best structure solution (that with the lowest R_{wp}) corresponded to an $R_{wp} = 6.4\%$, whereas R_{wp} was typically 16–18% for other structures calculated in the grid search procedure. This structure, with the chlorothalonil molecule lying parallel to the ab plane with atoms in the $2x,x,-z$ positions, was taken as the starting model for Rietveld refinement. The final refinement agreement factors and refined unit cell parameters are given in Table 1, and the final profile fit is shown in Figure 2. This disordered structure was later confirmed by single-crystal X-ray diffraction studies (details given in Table 1) and subsequent discussion of the experimental form 2 structure is based on the single-crystal results.

As it is currently not possible to accurately calculate the lattice energy of disordered structures, a second structure determination was attempted using an ordered model in the most basic symmetry (P1). The rhombohedral setting of this cell was used as a basis for the triclinic cell, with subsequent structure determination carried out using the Monte Carlo method^{13a} and Rietveld refinement (Table 1). Despite obtaining a good profile fit, this resulted in a structure that was implausible in terms of intermolecular packing and was rejected as a possible ordered approximation to the disordered structure of form 2.

Rietveld Refinement. All structures were refined using the GSAS program package,²¹ with the positions of all atoms refined subject to standard geometrical restraints on interatomic bond lengths and angles, and additional symmetry constraints imposed for form 2. Isotropic atomic displacement parameters were also refined, but constrained according to atom type or environment (i.e., Cl, N, aromatic or cyano C). Refinement of a preferred orientation parameter was also required for form 2.

Crystal Structure Prediction. The computer modeling was based on a rigid chlorothalonil molecule, using a molecular geometry obtained by ab initio optimization of the SCF wave function calculated with a 6-31G* basis set using the program CADPAC.²² The use of an ab initio molecular structure in the search for the other polymorphic forms avoids any bias from any packing effects on the molecular structure within form 1.

- (14) Sheldrick, G. M. *SHELXS-86: Program for Crystal Structure Solution*; University of Göttingen, Germany: Göttingen, Germany, 1986.
 (15) Sheldrick, G. M. *SHELXL-93: Program for Crystal Structure Refinement*; University of Göttingen, Germany: Göttingen, Germany, 1993.
 (16) Shirley, R. A. *CRYSFIRE Suite of Programs for Indexing Powder Diffraction Patterns*; University of Surrey: Surrey, U.K., 2000.
 (17) DeWolff, P. M. *J. Appl. Cryst.* **1968**, *1*, 108.

- (18) Seaton, C. C.; Tremayne, M. *POSSUM: Programs for Direct-Space Structure Solution from Powder Diffraction Data*; University of Birmingham: Birmingham, U.K., 2002.
 (19) Preferred orientation arises when crystallites have a tendency to align along a certain direction, resulting in a nonrandom distribution of crystallite orientations in the sample, affecting the relative intensities of given peaks. This is often most severe when the morphology is strongly anisotropic (e.g., flat plates or long needles), and the effects are often seen by comparison of the relative intensities of peaks in data collected in both disc and capillary geometries. The preferred orientation effects of platelike crystallites can be minimized by collection in capillary mode.
 (20) Aakeroy, C. B.; Beatty, A. M.; Rowe, D. M.; Seaton, C. C.; Tremayne, M. *Cryst. Growth Des.* **2001**, *1*, 377.
 (21) Larson, A. C.; Von Dreele, R. B. Report No. LAUR-86-748; Los Alamos National Laboratory: Los Alamos, NM, 1987.
 (22) Amos, R. D.; with contributions from Alberts, I. L.; Andrews, J. S.; Colwell, S. M.; Handy, N. C.; Jayatilaka, D.; Knowles, P. J.; Kobayashi, R.; Koga, N.; Laidig, K. E.; Laming, G.; Lee, A.; Maslen, P. E.; Murray, C. W.; Rice, J. E.; Simandiras, E. D.; Stone, A. J.; Su, M. D.; Tozer, D. J. *CADPAC6: The Cambridge Analytical Derivatives Package*, 6.0th ed.; Cambridge University, U.K., 1995.

Table 2. Reproductions of the Crystal Structures of Forms 1 and 3 of Chlorothalonil by Lattice Energy Minimization, Using the Model Potentials FIT and ANI and Either the Experimental X-ray (Exptl) or the Ab Initio Optimized Molecular Structure

model potential molecular structure	exptl exptl (ref 3)	FIT exptl	ANI exptl	FIT ab initio	ANI ab initio
Form 1 Space Group $P2_1/a$ Throughout					
$U_{\text{lat}}/\text{kJ mol}^{-1}$	-109.1 ^a	-110.12	-100.65	-109.72	-99.41
Structural Differences $\Delta(\text{calcd}-\text{exptl})$					
$a/\text{\AA}$	24.753	-0.409	+0.018	-0.335	+0.081
$b/\text{\AA}$	6.226	+0.038	+0.056	+0.025	+0.050
$c/\text{\AA}$	6.340	+0.002	-0.076	+0.027	-0.054
β/deg	95.41	+0.38	+1.35	+0.22	+1.29
cell vol/ \AA^3	972.719	-10.549	-4.665	-5.682	0.229
$\rho/\text{g cm}^3$	1.816	+0.020	+0.009	+0.010	-0.001
rms % cell ^b		1.017	0.866	0.851	0.702
Form 3 Space Group $P2_1$ Throughout					
$U_{\text{lat}}/\text{kJ mol}^{-1}$		-109.15	-99.84	-108.44	-99.19
Structural Differences $\Delta(\text{calcd}-\text{exptl})$					
$a/\text{\AA}$	13.5906	-0.0916	-0.1887	+0.2552	-0.1837
$b/\text{\AA}$	6.3033	-0.1673	-0.0497	-0.3699	-0.0501
$c/\text{\AA}$	18.4287	-0.0421	+0.1113	-0.1650	0.0536
β/deg	109.45	-3.04	-0.04	-5.46	-0.17
cell vol/ \AA^3	1488.613	-27.682	-23.051	-32.678	-26.03
$\rho/\text{g cm}^3$	1.780	+0.033	+0.028	+0.039	+0.032
rms % cell ^b		1.59	0.99	3.59	0.92

^a Experimental heat of sublimation of unspecified form of chlorothalonil from NIST Web Book.³⁶ ^b rms % errors in the cell lengths.

Table 3. Five Lowest-Energy Crystal Structures for Chlorothalonil Found in the MOLPAK Search and Minimized in DMAREL Using the ANI Potential

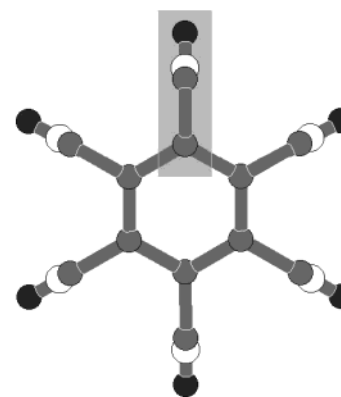
	space group	$E_{\text{lat}}/\text{kJ/mol}$	cell vol/ \AA^3	$a/\text{\AA}$	$b/\text{\AA}$	$c/\text{\AA}$	α/deg	β/deg	γ/deg
exptl	$P2_1/a$	-98.79	243.180	24.753	6.226	6.340	90.00	95.41	90.00
min ^a	$P2_1/a$	-99.40	243.246	24.840	6.272	6.288	90.00	96.65	90.00
Structures Found in Search			Reduced Cell Parameters						
FC45	$P2_1/c$	-99.40	243.243	6.272	6.288	24.839	96.65	90.00	90.00
AB15	$P1$	-99.39	238.424	6.482	7.774	10.166	91.31	106.80	102.50
AI44	$P2_1/c$	-99.31	243.379	6.228	12.309	12.750	95.12	90.00	90.00
AF18	$P2_1$	-99.02	243.922	6.235	6.302	12.468	95.31	90.00	90.00
AB3	$P1$	-98.16	243.514	6.077	6.350	12.727	94.53	94.72	92.96

^a Min is the experimental crystal structure minimized using the ANI model with ab initio optimized molecular structure and therefore represents the closest to the experimental structure that could be found in the search.

Table 4. Final Refined Parameters and Agreement Factors for the Single-Crystal Structure of Chlorothalonil Form 3 and Those from Rietveld Refinement of the Predicted AF18 and AI44 Structures

	single-crystal	powder (AF18)	powder (AI44)
$a/\text{\AA}$	13.591(2)	12.4281(5)	12.6674(12)
$b/\text{\AA}$	6.3033(9)	6.2426(2)	6.2441(5)
$c/\text{\AA}$	18.429(3)	6.2918(2)	12.4566(10)
α/deg	90	90	90
β/deg	109.448(5)	94.033(2)	94.320(5)
γ/deg	90	90	90
vol/ \AA^3	1488.6(4)	486.93(5)	982.49(15)
space group	$P2_1(4)$	$P2_1(4)$	$P2_1/c(14)$
Z	6	2	4
R_{wp}	0.0696 (R)	0.0341	0.0574
R_{p}		0.0232	0.0373
R_{F2}	0.1318 (R_{w})	0.2375	0.2807
χ^2		5.24	6.94

The electrostatic contribution to the lattice energy was modeled accurately throughout, using sets of atomic multipoles derived from a distributed multipole analysis²³ (DMA) of the molecular charge distribution calculated at the MP2 level with 6-31G* basis set. All terms in the atom-atom multipole expansion of the electrostatic energy up to R_{ik}^{-5} were included in the intermolecular lattice energy. The other contributions cannot be modeled so reliably, and hence, two contrasting

**Figure 1.** Disordered structural model of the chlorothalonil molecule used for powder structure solution of form 2. Carbon atoms are shown in gray, chlorine in white, and nitrogen in black, with a C-(C≡N)/Cl spur highlighted.

models were used. The first model, used in the search for low-energy structures, had C, N, and Cl isotropic atom-atom repulsion-dispersion parameters that had been empirically derived by fitting to crystal structures and some heats of sublimation of azahydrocarbons²⁴ and perchlorohydrocarbons.²⁵ This model potential has the functional form:

(24) Williams, D. E.; Cox, S. R. *Acta Crystallogr., Sect. B* **1984**, *40*, 404.

(25) Hsu, L.-Y.; Williams, D. E. *Acta Crystallogr., Sect. A* **1980**, *36*, 277.

(23) Stone, A. J.; Alderton, M. *Mol. Phys.* **1985**, *56*, 1047.

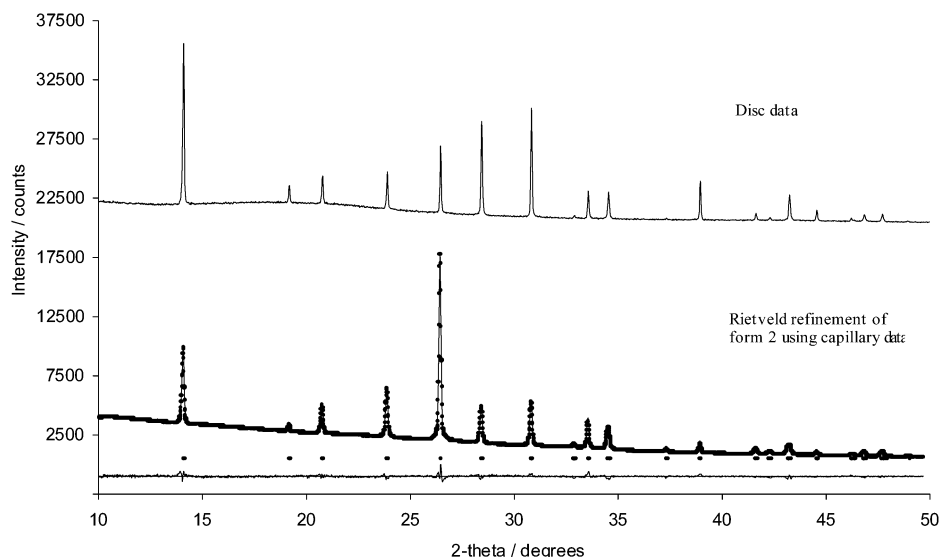


Figure 2. X-ray powder diffraction patterns recorded for chlorothalonil form 2 collected with the sample packed in a disk (top) and for the final Rietveld refinement of form 2 using data recorded in capillary geometry (bottom). Observed (marks), calculated (solid line), and difference (below) profiles are shown, and reflection positions are also marked.

$$U = \sum_{i \in 1, k \in 2} U_{ik} = \sum_{i \in 1, k \in 2} (A_{it} A_{k\kappa})^{1/2} \exp[-(B_u + B_{kk})R_{ik}/2] - \frac{(C_u C_{kk})^{1/2}}{R_{ik}^6} + U_{\text{elec}}(\text{DMA}, \Omega_{ik}, R_{ik}^{-5}; n \leq 5)$$

where atom i (in molecule 1 of type t) and atom k (in molecule 2 of type κ) are separated by a distance R_{ik} and have a relative orientation Ω_{ik} , defined by the intermolecular unit atom–atom vector and the intramolecular bonds. This total model potential, where the non-electrostatic terms are empirical, is denoted FIT. It assumes that the repulsive wall around all atoms is spherical and also that the parameters can be transferred from different classes of molecules, with the heteroatomic interactions estimated by the combining rules.

To dispense with these assumptions, we also developed an anisotropic atom–atom potential, with the form:

$$U = \sum_{i \in 1, k \in 2} A_{ik} \exp\{-B_{ik}[R_{ik} - \rho_{ik}(\Omega_{ik})]\} - C_{ik}/R_{ik}^6 + U_{\text{elec}}(\text{DMA}, \Omega_{ik}, R_{ik}^{-n}; n \leq 5)$$

This ANI model potential uses the same DMA electrostatic model, but the dispersion is estimated by a Slater–Kirkwood atom–atom C_6 dispersion model²⁶ using atomic polarizabilities.²⁷ The main innovation in this potential is that the intermolecular effects of the nonspherical features in the atomic charge distributions, such as the chlorine lone pair density and the nitrogen triple bond, can be represented in the repulsion as well as in the electrostatic contribution. The repulsion model is based on the assumption that the repulsion is proportional to the overlap of the molecular charge density.¹⁰ The SCF ab initio charge density of chlorothalonil is divided into atomic contributions, allowing the intermolecular overlap, readily calculated by GMUL,²⁸ to also be divided into its contribution from each intermolecular pair of atoms. By calculating the overlap at many different relative orientations of the two molecules, sets of atom–atom overlaps as a function of R_{ik} and Ω_{ik} are generated. These are fitted to establish the transferability, anisotropy, and parameters of an analytic model for the overlap. In the

case of chlorothalonil, the aromatic carbons and the cyano carbons warranted separate parameters, but could be modeled as isotropic, and the Cl and N atom overlaps could be well-represented by a constant anisotropic shape consistent with the traditional view of their valence electron density. The proportionality constant between the analytical model for the overlap and the repulsion potential was obtained by optimizing the reproduction of the cell volume³ of chlorothalonil form 1. Additional mathematical details and the potential parameters are given in the Supporting Information.

The crystal structure prediction search used an updated version of MOLPAK²⁹ to generate dense packings of the ab initio molecular structure of chlorothalonil in 29 common organic crystal coordination geometries, which are in the space groups, $P1$, $P\bar{1}$, $P2_1$, $P2_1/c$, Cc , $C2$, $C2/c$, $P2_12_1$, $Pca2_1$, $Pna2_1$, $Pbcn$, and $Pbca$. A total of 1304 MOLPAK starting structures were then used as starting points for minimizing the lattice energy, calculated using the FIT potential in the latest version of DMAREL.³⁰ The crystallographic symmetry was conserved in the minimization, and it was lowered if this resulted in a stationary point rather than a true minimum. The most energetically favorable structures, those within 5 kJ/mol of the global minimum, were then reminimized using the ANI potential. The elastic constant tensor for each hypothetical structure was then calculated from the second derivative matrix.³¹

The morphology of each of the low-energy structures and relative growth rates were estimated using the attachment energy model.³² This assumes that the growth rate of each face is proportional to the energy released when a growth layer is added to that face (the attachment energy). This is a reasonable approximation for vapor-grown crystals below the roughening temperature.³³ The FIT potential, with charge-equilibration charges replacing the DMA electrostatic model, was used for calculating the morphology in Cerius² software.³⁴

Results and Discussion

Computational Prediction of Polymorphism. Both the empirical transferable potential FIT and the specific potential ANI reproduce the crystal structure of form 1 (Table 2) well within the errors usually associated with comparing lattice

(26) Slater, J. C.; Kirkwood, J. G. *Phys. Rev.* **1931**, *37*, 682.

(27) Miller, K. J. *J. Am. Chem. Soc.* **1990**, *112*, 8533.

(28) Wheatley, R. J. *GMUL 3s*, An extension to the GMUL program (version 3) that calculates an analytical form for the overlap of distributed charge densities; University of Nottingham: Nottingham, U.K., 1997.

(29) Holden, J. R.; Du, Z. Y.; Ammon, H. L. *J. Comput. Chem.* **1993**, *14*, 422.

(30) Willock, D. J.; Price, S. L.; Leslie, M.; Catlow, C. R. A. *J. Comput. Chem.* **1995**, *16*, 628.

(31) Day, G. M.; Price, S. L.; Leslie, M. *Cryst. Growth Des.* **2001**, *1*, 13.

(32) Berkovitch-Yellin, Z. *J. Am. Chem. Soc.* **1985**, *107*, 8239.

(33) Hartman, P.; Bennema, P. *J. Cryst. Growth* **1980**, *49*, 145.

(34) *Cerius2*; Molecular Simulations Inc.: San Diego, CA, 1997.

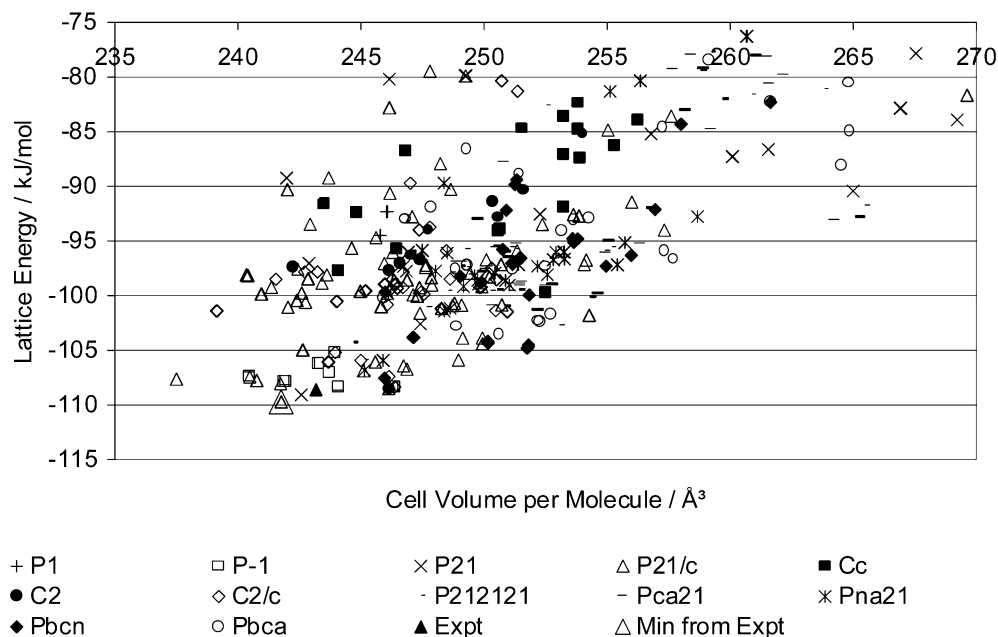


Figure 3. Plot of minima in the lattice energy of chlorothalonil found in the MOLPAK/DMAREL search using the FIT model potential. The minima are denoted by the space group of the starting structure generated by MOLPAK. In some cases, the corresponding minimum was of a lower symmetry.

energy minima with room-temperature crystal structures.³⁵ The lattice energy calculated by the FIT potential is remarkably close to the experimental sublimation energy of -109.1 kJ/mol,³⁶ even considering that the potential had been fitted to sublimation energies. The specific nonempirical potential ANI, which was constructed without using any energy information, predicts the lattice energy to within 10 kJ/mol, well within the error normally allowed considering the approximations implicit in comparing calculated lattice energies with experimental heats of sublimation.³⁷ The differences in the lattice energy minima according to whether the experimental molecular structure or the idealized ab initio molecular structure was used are very small. This is in accord with the very small asymmetry in the experimental structure and the minor differences from the ab initio molecular model. Hence, the ab initio molecular model and either potential are suitable for modeling the crystal structures of chlorothalonil, although after the discovery of form 3, it was found to be somewhat better reproduced by the specific nonempirical potential.

Figure 3 plots the minimized lattice energies against the cell volume per molecule for the hypothetical structures found in the MOLPAK/DMAREL search. Approximately one third of the minimizations resulted in a lower symmetry space group than the starting structure. The 27 structures within 5 kJ/mol of the global minimum were reminimized with the ANI potential, resulting in the structures given in the Supporting Information, with the five lowest-energy structures shown in Table 3. The change in potential produced some reordering of the relative lattice energies. It also reduced the number of distinct structures to 22, as some structures that were distinct minima with FIT converged to the same minima for the ANI potential surface,

in some cases lowering the symmetry. However, for both potentials, the global minimum found in the search corresponded to form 1, with cell parameters corresponding to the minimum in Table 2.

A few of the predicted low-energy structures can be eliminated as plausible polymorphs of chlorothalonil by consideration of mechanical properties and relative growth rates. The elastic constants of most of the hypothetical structures and the known experimental structures were within the range of 10–30 GPa for the stiffness to compression (C_{11} , C_{22} , and C_{33}) and up to about 15 GPa for the shear constants (C_{44} , C_{55} , and C_{66}). Two crystal structures, AB11 and AM12, were predicted to have a very low resistance to shear, lower than known unusually deformable organic crystal structures,⁸ and thus they appear improbable as polymorphs. The estimated elastic constants for all three forms are provided in the Supporting Information, as industrially useful for process modeling. The other structures, including the sheet structures, all had reasonable mechanical properties for organic crystals,³⁸ though the anisotropy in the elastic tensor reflected the packing.

In agreement with experimental observations, the predicted morphology of form 1 was a rectangular plate, and even the slowest growing face (200) had a reasonable growth rate with an attachment energy of -17.5 kJ/mol. A few of the hypothetical structures, AB36, AB37, and AK17, had more equant predicted morphologies, with aspect ratios around 2 to 3 and higher attachment energies (up to 30 kJ/mol) for their slowest growing face.

However, most hypothetical structures were also predicted to have platelike morphologies, with the largest dimension up to 10 times the thickness. The prediction of structures with such anisotropic morphologies provides a warning that preferred orientation is likely to be a problem in a subsequent powder diffraction study and in this case could be addressed by initial

(35) Beyer, T.; Price, S. L. *CrystEngComm* **2000**, *34*, 183. <http://www.rsc.org/CrystEngComm>.

(36) Chickos, J. S. Heat of Sublimation Data. In *NIST Chemistry WebBook, NIST Standard Reference Database*; Mallard, W. G., Linstrom, P. J., Eds.; National Institute of Standards and Technology: Gaithersburg, MD, 1998; Vol. 69. <http://webbook.nist.gov>.

(37) Gavezzotti, A. Crystal Symmetry and Molecular Recognition. In *Theoretical Aspects and Computer Modeling of the Molecular Solid State*; Gavezzotti, A., Ed.; John Wiley & Sons: Chichester, U.K. 1997; Vol. 1, p 97.

(38) Day, G. M.; Price, S. L. Properties of Crystalline Organic Molecules; In *Handbook of Elastic Properties of Solids, Liquids and Gases*; Levy, M., Bass, H. E., Stern, R. R., Eds.; Academic Press: San Diego, CA, 2001; Vol. III, p 3.

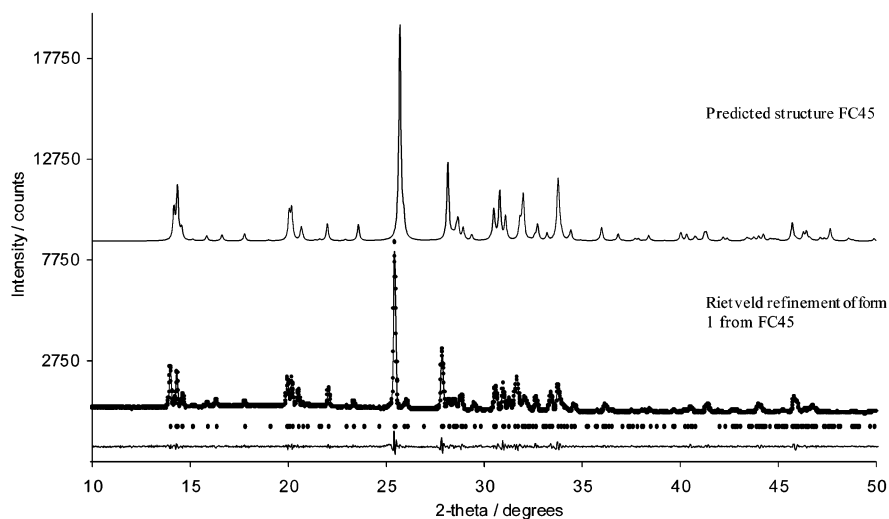


Figure 4. X-ray powder diffraction data simulated for the predicted structure FC45 (top) and after Rietveld refinement (bottom). Observed, calculated, and difference profiles as in Figure 2. Final Rietveld agreement factors: $R_{wp} = 7.56\%$, $R_p = 5.81\%$, $R_{F2} = 10.11\%$, $\chi^2 = 1.99$, $a = 24.797(1)$ Å, $b = 6.2398(3)$ Å, $c = 6.3482(3)$ Å, $\beta = 95.416(2)^\circ$.

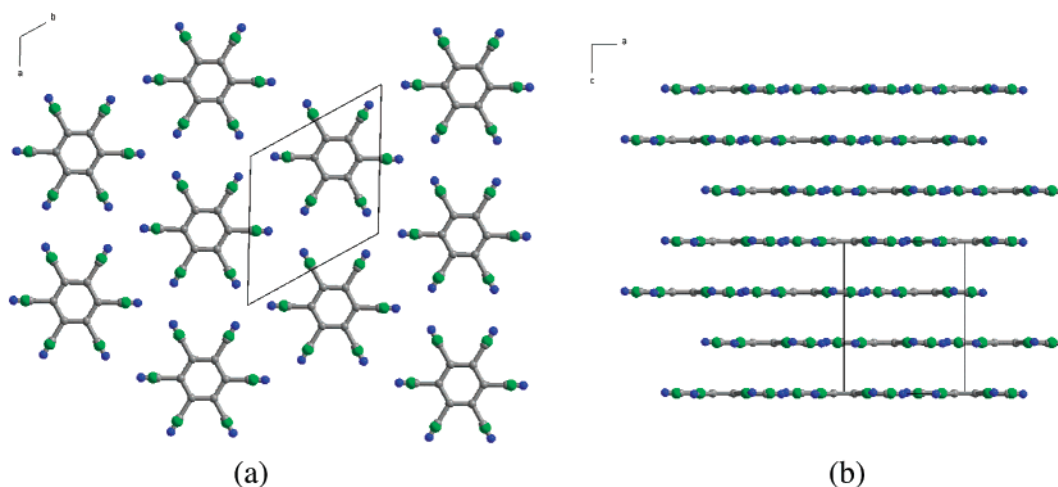


Figure 5. View of the $R\bar{3}m$ disordered crystal structure of chlorothalonil form 2 showing (a) a single layer in the (110) plane and (b) stacking of these layers in the [001] direction. Carbon atoms are shown in gray, chlorine in green, and nitrogen in blue.

data collection in capillary geometry.¹⁹ Three structures, AM12, DC35, and DD42, were predicted to be extremely platelike, with attachment energies for their dominant face of less than 0.5 kJ/mol and aspect ratios of over 40. These morphologies are so extreme, and the growth rates predicted by the attachment energy model so slow relative to other hypothetical structures, that they can also be eliminated as plausible polymorphs.

Although a number of structures have been identified as improbable polymorphs in terms of physical characteristics, there are still many structures that appear as possible polymorphs of chlorothalonil (Table 3 and Supporting Information). There are two structures based on the same layer structure, which is virtually isoenergetic with form 1 when the layers are stacked with a 3-fold displacement (i.e., molecules in layers 1 and 4 are above each other) (AB15), and only 1.2 kJ/mol less stable when there is a 6-fold displacement of the layers (AB3) (Table 3). With the FIT potential, the relative stability of these two structures is reversed and the energy gap relative to the global minimum increased, but only to 1.9 and 2.3 kJ/mol. Therefore, both potential models suggest that this layer structure is very competitive energetically with the observed stable form 1. The

other two structures that are particularly energetically favorable (Table 3), AI44 and AF18, have considerable similarities in their close contacts to form 1, but are based on single herringbone packing, rather than a double herringbone.

Crystal Structures of Polymorphic Forms from X-ray Diffraction and Prediction. (i) **Form 1.** It is clear that the simulated powder diffraction pattern for structure FC45 differs only slightly from the experimental data collected for form 1, and hence, this predicted structure proved to be an adequate starting model for a successful restrained Rietveld refinement (Figure 4).

(ii) **Form 2.** The disordered structure of form 2, determined from both single-crystal and powder X-ray diffraction data, consists of infinite planar sheets in which each molecule is surrounded by six others, with π - π stacking of these layers (running parallel to the (001) plane) to form a three-dimensional structure (Figure 5a,b).

Since it is not currently possible to calculate reliable lattice energies for disordered structures, the hypothetical low-energy structures found in the computational search were studied to determine whether any were comparable to the new form 2

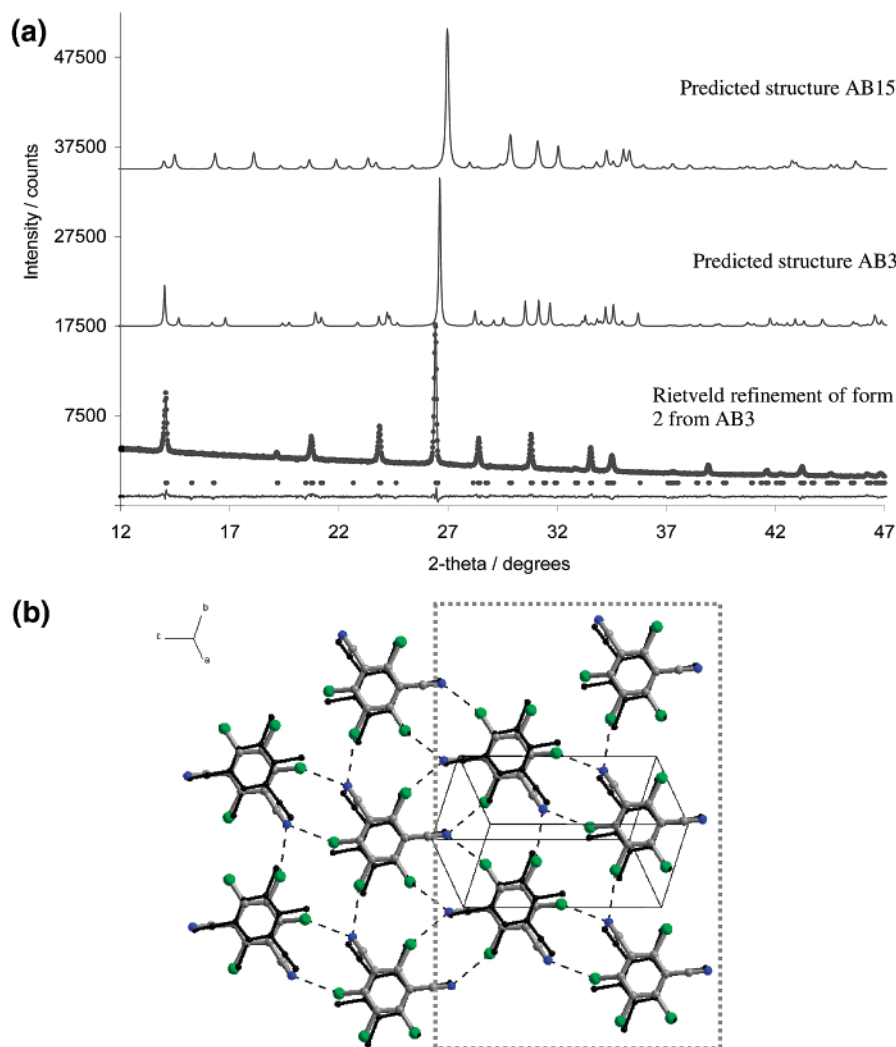


Figure 6. (a) X-ray powder diffraction data simulated for the predicted structures AB15 (top) and AB3 (middle) and AB3 after Rietveld refinement (bottom); as in Figure 2. (b) The crystal structure of AB3 before refinement (black atoms and bonds) and after refinement (atoms depicted as in Figure 5; short C=N...Cl contacts are indicated by dashed lines). An antiparallel ribbon running perpendicular to [001] within the layer is also highlighted.

structure. AB15 and AB3 were found to contain a similar layer structure, although only AB3 shows a similar displacement of these layers to the experimental structure. Comparison of the simulated powder diffraction data for AB3 and the experimental data for form 2 also shows good agreement (Figure 6a). The AB3 structure was used as a starting point for Rietveld refinement against the experimental form 2 data to establish if it could be considered as an ordered approximation to the disordered $R\bar{3}m$ structure. By application of similar constraints to those used in the original powder refinement, a successful refinement was achieved (Figure 6a), with final agreement factors given in Table 1, confirming that the refined AB3 structure is a good ordered representation of form 2. Although AB15 contains a similar layer structure, the displacement of these layers is not comparable to the form 2 structure in all directions. The simulated powder data for AB15 shows more significant differences from the experimental data and not surprisingly resulted in unsuccessful attempts at Rietveld refinement.

Figure 6b shows the positions of the molecules in a single layer in the AB3 structure before and after refinement. It is clear that refinement has caused a slight rotation of the molecule within the plane of the layer (parallel to the (111) plane),

resulting in a shift from triclinic toward a higher “hexagonal-type” symmetry. The interlayer distance of the refined AB3 structure (3.31(1) Å) is also comparable to the single-crystal experimental structure (3.364(6) Å). Rotation of the molecule in 60° steps within the (111) plane generated five new crystal structures that were indistinguishable by R_{wp} , confirming that any of the six orientations give an equivalent representation of the disordered structure. This $P\bar{1}$ structure contains a rational network of intermolecular interactions and can be regarded as a good ordered approximation to the disordered crystal structure of form 2. The disorder could occur either through the existence of domains of the ordered $P\bar{1}$ structure rotated through all six possible orientations in the crystal or from disorder in the orientation and offsets in the stacking of complete ordered layers.

The predicted morphology of AB3 is clearly platelike, with the aspect ratio being predicted to be twice that of form 1. The anisotropic morphology of form 2 gives rise to the severe preferred orientation observed in the powder diffraction data. In both the disordered and ordered descriptions of this structure, the molecules lie in planar sheets, parallel to (001) and (111) in $R\bar{3}m$ and $P\bar{1}$, respectively, and correspond to the direction

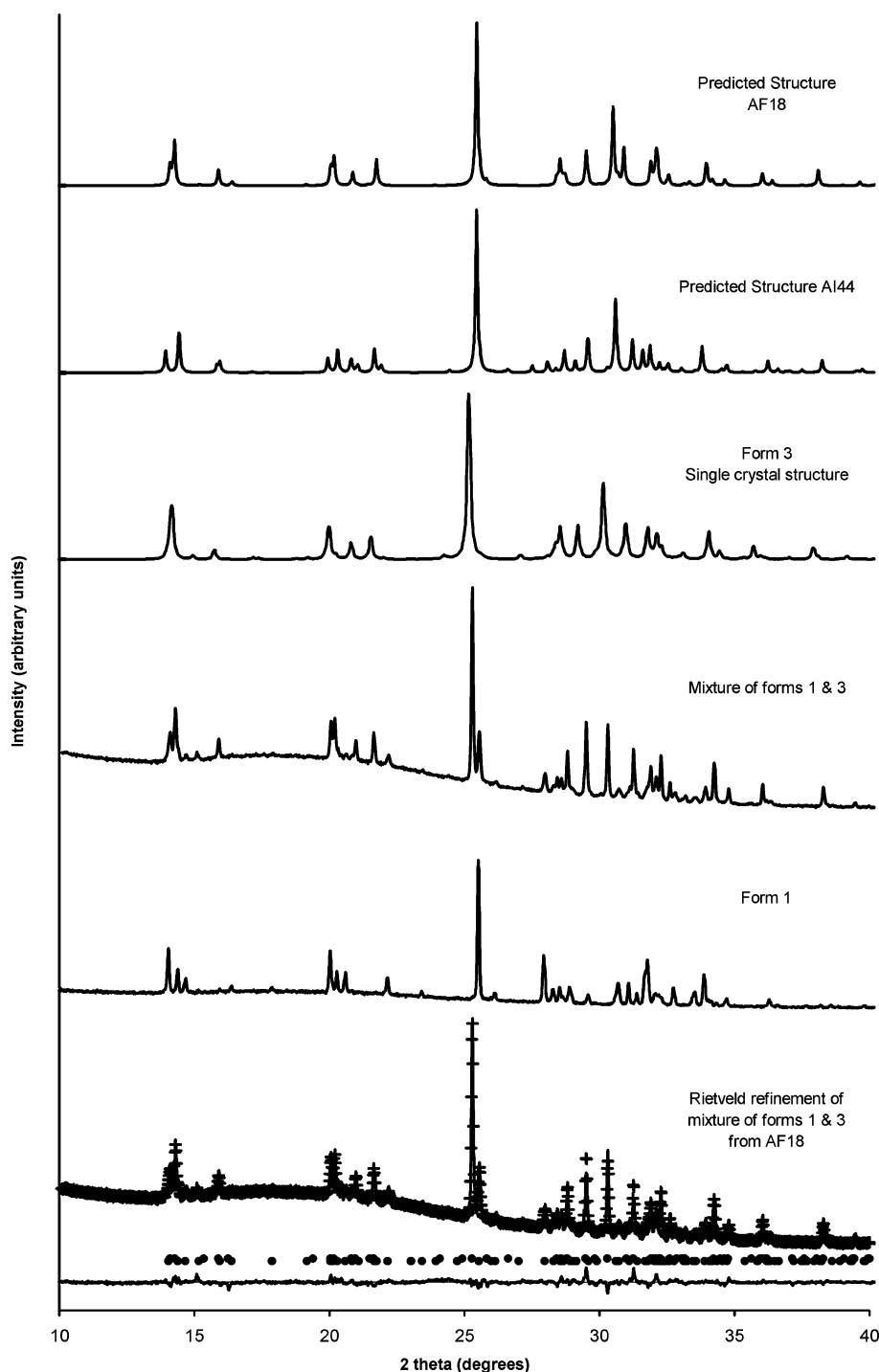


Figure 7. Comparison of the simulated powder diffraction patterns of the single-crystal structure of form 3 and the predicted structures AF18 and AI44 and the experimental data for pure form 1 and the mixture of forms 1 and 3 (including after Rietveld refinement).

of the preferred orientation correction used in each structure refinement (Table 1).

(iii) Form 3. The powder diffraction pattern of form 3 clearly shows that the bulk material is a mixed phase with form 1. Comparison of the simulated powder diffraction data for the two remaining structures that were highlighted as being particularly energetically stable, AI44 and AF18, both showed significant agreement with the form 3 pattern (Figure 7). As both structures also show great similarities, separate Rietveld refinements were attempted using each structure as a starting

model, and in both cases, a two-phase refinement was carried out to account for the presence of form 1. The refinement of AF18 progressed well (as shown by the Rietveld agreement factors in Table 4 and the quality of the profile fit); however, close inspection of the fit reveals that there is some discrepancy between the structural model and the experimental data. Although the errors on the difference plot are small, the deficiencies of this structural model are clearly demonstrated by the poor value of R_F^2 . Refinement of the AI44 structure resulted in a slightly worse profile fit (Table 4). The discrep-

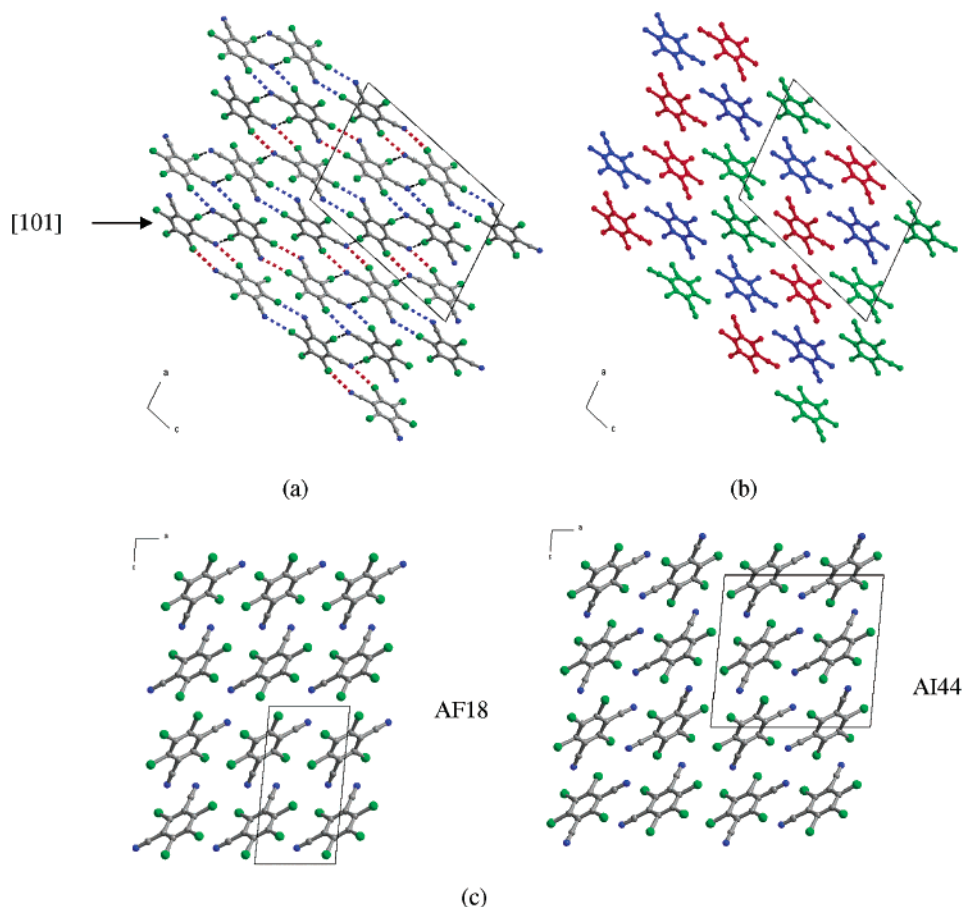


Figure 8. Crystal structure of chlorothalonil form 3 shown in projection down the b -axis with (a) the $[101]$ direction marked and the $C\equiv N\cdots Cl$ interactions indicated by dashed lines (blue shows the clockwise and red the anticlockwise spirals; other interactions are in black). (b) Each symmetry-independent molecule indicated (red, green, and blue molecules). (c) The structures of AF18 and AI44, each shown in projection down the b -axis.

ancies between these two Rietveld fits are similar to those that might arise from disorder (cf. in form 2), however, subsequent single-crystal analysis showed that this was not the case with form 3.

The crystal structure of form 3 has three independent molecules in the asymmetric unit (Figure 8a,b), differing from both the AF18 and AI44 structures used for Rietveld refinement and any of the predicted polymorphs given in Table 3. Indeed, with multiple molecules in the asymmetric unit, this structure lies outside the capabilities of current crystal structure prediction calculations. This new polymorph has a single herringbone structure in which the molecules form alternating opposing intermolecular spirals running parallel to the b -axis. These spirals combine to form infinite sheets in the (011) plane, which are in turn linked into a complicated three-dimensional structure (Figure 8a).

Although the structure of form 3 is clearly different from the predicted structures AF18 and AI44, there are also significant similarities between these three structures (and their simulated powder diffraction patterns, Figure 7); all have a single herringbone structure in which the relative positions and orientations of the molecules are identical, with only the position of the $C\equiv N$ or Cl substituents varying. For example, in the $[100]$ direction, the AF18 structure forms a chain of molecules that are related by translation, whereas in AI44 a similar chain is formed in which the molecules are related by inversion (Figure

8c), resulting in a “flip” of alternate molecules within this chain. In both cases, the chains are then related by 2_1 screw axes to neighboring chains running perpendicular to the c -axis. Although the relationship between the molecules in the form 3 structure is much more complex, a similar chain of molecules can be viewed in the $[101]$ direction related by a pseudo-symmetry combination of the elements in AF18 and AI44, with other chains again generated by 2_1 screw axes. In effect, form 3 can be considered as a combination of the AF18 and AI44 structures, or conversely, the predicted structures can be considered as good approximations to the experimental form 3 structure. This relationship is enhanced further in that the lattice energy of form 3, calculated with the ANI potential (Table 2), actually lies between the calculated energies of AF18 and AI44 and within 0.2 kJ/mol of either (Table 3).

Structural Comparison of Forms 1, 2, and 3. The crystal structures of all three forms of chlorothalonil are based on infinite molecular chains that are linked either into linear antiparallel ribbons or infinite sheets. The antiparallel ribbons found in form 1 have a similar intermolecular network to sections within each layer in the $P\bar{1}$ ordered approximation of form 2 (Figure 6b). In form 2, these ribbons are linked together generating an infinite flat sheet, whereas in form 1 the ribbons interact to form a double herringbone structure. The puckered chains in form 3 are linked into a single herringbone structure through a complex set of interactions.

Conclusions

A combination of both single-crystal and X-ray powder diffraction techniques and crystal structure prediction has been used to characterize and rationalize the structures of three polymorphs of chlorothalonil. The theoretical structure prediction successfully located the global minimum sufficiently close to the structure of form 1 to allow straightforward Rietveld refinement. The use of two potentials, derived in very different ways, provides more confidence that form 1 is the thermodynamically favored structure at low temperatures. The structure of a new disordered polymorph, form 2, was solved and refined from powder diffraction data. Although the disorder in the layer stacking could not be predicted by current computational methods, a low-energy structure found in the computational search to be almost as stable as form 1 provided a reasonable ordered approximation to the structure of form 2 and was refined against the experimental powder data. This ordered layer structure provides a valuable insight into the nature of the disorder that could not be obtained from diffraction data alone and clearly demonstrates how the complementary use of these two techniques can reveal structural information that would be unavailable if the experimental and theoretical results were considered independently. Single-crystal diffraction was used to determine the structure of form 3, another new polymorph with a complex structure containing three independent molecules in the asymmetric unit. Although this $Z' > 1$ structure also lies outside the current capabilities of crystal structure prediction, we identified two theoretical low-energy structures that show

significant similarities to form 3, both in terms of lattice energy and molecular packing, and contain structural elements that can be combined to generate the experimental structure. The possibility that polymorphs relating directly to AF18 and AI44 or an ordered version of form 2 may occur and that other low-energy structures predicted by both potentials might correspond to as yet undiscovered polymorphs is currently being investigated through further solvent screening and variation of crystallization conditions.

Acknowledgment. This research was supported by Glaxo-SmithKline through a studentship to C.C.S. and by the Royal Society through the award of a University Research Fellowship to M.T. We are grateful to Avecia and AstraZeneca for funding H.H.Y.T. through the Zeneca Strategic Research Fund. Graeme Day, Maurice Leslie, and John Mitchell are thanked for assistance with the computational work.

Supporting Information Available: X-ray crystallographic data for the structure determinations of forms 2 and 3 (CIF). Mathematical details and potential parameters for the crystal structure prediction calculations, the 22 lowest-energy crystal structures for chlorothalonil generated in the search, with their ANI potential lattice energies, densities, and reduced cell constants, and the predicted elastic constants for the polymorphs of chlorothalonil (PDF). This material is available free of charge via the Internet at <http://pubs.acs.org>.

JA0498235